Polymer 51 (2010) 6107–6114

Contents lists available at ScienceDirect

Polymer

journal homepage: www.elsevier.com/locate/polymer

Cross-linked polymers based on 2,3,5,6-tetra-substituted pyrrolo[3,4-c]-pyrrole-1,4(2H,5H)-dione (DPP): Synthesis, optical and electronic properties

Kai Zhang [a], Bernd Tieke [a,*], John C. Forgie [b], Filipe Vilela [b], John A. Parkinson [b], Peter J. Skabara [b]

[a] Department of Chemistry, University of Cologne, Luxemburger Str. 116, D-50939 Cologne, Germany
[b] WestCHEM, Department of Pure and Applied Chemistry, University of Strathclyde, Glasgow G1 1XL, UK

ARTICLE INFO

Article history:
Received 17 August 2010
Received in revised form
26 October 2010
Accepted 28 October 2010
Available online 3 November 2010

Keywords:
Pyrrolo[3,4-c]pyrrole-1,4(2H,5H)-dione
DPP
Electropolymerization

ABSTRACT

A series of 2,3,5,6-tetra-substituted pyrrolo[3,4-c]pyrrole-1,4(2H,5H)-dione (DPP) derivatives carrying thienyl-, 3,4-ethylenedioxy-thienyl- (EDOT-) and 3,4-ethylenedithiathienyl- (EDTT-) substituent groups have been synthesized and electrochemically polymerized. The polymers were investigated using UV/vis absorption spectroscopy and cyclic voltammetry. It was found that the growth of the polymers proceeded as random coupling of the thiophene groups in the 2-,3-,5-, and 6-positions of the DPP chromophore. In the cross-linked polymers, conjugated sequences were only built through coupling of thiophene groups in 3,6-positions, and separated by non-conjugated sequences through coupling with thiophene units in other positions of the DPP core.

1. Introduction

Conjugated polymers and oligomers have gained much attention due to their interesting optical and electronic properties, and their potential application in light emitting diodes [1,2], solar cells [3,4], field effect transistors [5–7], sensors [8], and electrochromic devices [9–12]. The incorporation of heterocyclic and heteroaromatic moieties into the conjugated polymer chain is a useful strategy to alter optical properties such as absorption and emission maxima, electronic properties such as band gap and oxidation potential, and ordering and π-stacking of the polymer chains [10].

3,6-Diphenyl-pyrrole[3,4-c]pyrrole-1,4-dione (DPP) and some of its derivatives represent red coloured, highly luminescent compounds, which are commercialised as high performance pigments and used in paints, colour inks and plastics [13,14]. Previous studies have shown that soluble DPP derivatives with deep colour and strong luminescence can be prepared upon alkylation of the lactam units [15–17]. If properly functionalised, alkylated and -arylated DPP monomers can be introduced into polymers prepared by Pd-catalysed arene–arene coupling reactions such as Suzuki, Stille, and Heck coupling [18–22]. These materials show intense red colours, strong red photoluminescence, and electroluminescence [23,24], which render them attractive as active materials in a variety of electronic devices. In our previous work, we reported the electropolymerization of bis-EDOT-substituted *N*-alkylated and -arylated DPP monomers [25,26]. It has been shown that the incorporation of a 2,3,5,6-tetraarylated DPP chromophore in a conjugated linear polymer chain via its 2- and 5- aryl units (i.e., the N-aryl units) results in non-π-conjugated polymers, whereas incorporation via the aryl units in the 3- and 6-positions results in π-conjugated polymers with a bathochromic shift of the optical absorption by about 120 nm (Fig. 1).

It was of great interest to study the electropolymerization and properties of deposited polymer films, in DPP monomers with electropolymerizable units such as thiophene derivatives attached to the phenyl groups in the 2-, 3-, 5- and 6-positions. In this work, we report the electropolymerization of a series of tetrafunctionalized DPP monomers with 4-hexyl-thiophene-, 3,4-ethylenedioxythiophene- (EDOT-) and 3,4-ethylenedithiathiophene- (EDTT-) groups attached to the 2-, 3-, 5-, and 6-positions of the DPP core (Fig. 2). We will study the mechanism of the polymer growth. Special emphasis is paid to differences of the coupling patterns between the 2,5- and 3,6-positions, and the optical and electrochemical properties of the cross-linked and the linear DPP polymers.

* Corresponding author. Tel.: +49 221 470 2440.
E-mail address: tieke@uni-koeln.de (B. Tieke).

0032-3861/$ – see front matter © 2010 Elsevier Ltd. All rights reserved.
doi:10.1016/j.polymer.2010.10.054

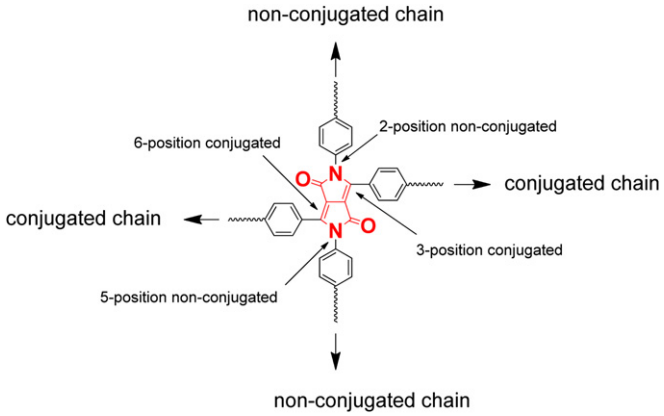

Fig. 1. Structure of 2,3,5,6-substituted DPP.

2. Experimental section

2.1. Chemicals

4′-Bromoacetophenone (**1**) was purchased from Aldrich. Ethyl 3-(4-bromophenyl)-3-oxopropanoate (**2**), diethyl 2,3-bis(4-bromobenzoyl)succinate (**3**), 3,6-bis(4-bromophenyl)furo[3,4-c]furan-1,4-dione (**4**) were synthesized according to previous procedures [15,27]. 4-Hexylthien-2-yl trimethylstannane (**7**), 3,4-ethylenedioxythien-2-yl trimethylstannane (**8**) and 3,4-ethylenedithiathien-2-yl trimethylstannane (**9**) were synthesized according to literature procedures [28,29]. All other chemicals and solvents were purchased from commercial sources and were used without further purification. Air- and/or water- sensitive reactions were conducted under nitrogen using dry solvents. Microwave assisted syntheses were carried out using a Biotage Initiator Sixty EXP Microwave System.

2.2. Physical measurements

NMR data were acquired on Bruker AVANCE III NMR spectrometers operating at 400.13 and 600.13 MHz for proton resonance and equipped with [^{1}H, ^{13}C, ^{19}F, ^{31}P]-QNP-z and BBO-z-ATM probeheads respectively. Data were acquired at 9.4 T and ambient temperature for samples solubilized in $CDCl_3$ (DPP1 and DPP3) and at 14.1 T and 350 K for samples solubilized in DMSO-d_6 (DPP2 and DPP3). 1D ^{1}H NMR data were acquired under typical single pulse acquire conditions. For the less soluble DPP2 and DPP3 samples 150 MHz 1D ^{13}C-{^{1}H} NMR data were acquired with 20×10^3 transients using a uniform driven equilibrium Fourier transform (UDEFT) approach according to Piotto et al. [30] in order to maximize the ^{13}C signal-to-noise ratio. 2D [^{1}H, ^{13}C] HSQC NMR data were acquired using a gradient selected sensitivity improved echo-anti echo approach in either standard or multiplicity edited modes. Chemical shifts were referenced internally to the residual solvent signal and are quoted in parts per million. Elemental analyses were obtained on a Perkin–Elmer 2400 elemental analyzer. Absorption spectra were measured on a Unicam UV 300 spectrophotometer.

2.3. Electrochemistry

Dichloromethane (HPLC grade, Aldrich), acetonitrile (HPLC grade, Aldrich) and tetra-*n*-butylammonium hexafluorophosphate ($TBAPF_6$, electrochemical grade, Fluka) were used as received. Electrochemical measurements were performed on a CH Instruments 660A electrochemical workstation with IR compensation using anhydrous dichloromethane or acetonitrile as the solvent, silver wire as the pseudo-reference electrode, and platinum wire and glassy carbon as the counter and working electrodes, respectively. Electrochemical data were referenced to the ferrocene/ferrocenium redox couple using the metallocene as an internal standard. All solutions were purged with Ar. The monomer concentrations were ca. 1×10^{-3} M, *n*-Bu_4NPF_6 (0.1 M) was used as the supporting electrolyte. Spectroelectrochemical experiments were conducted on ITO glass.

2.4. Monomer synthesis

2.4.1. 2,3,5,6-Tetrakis(4-bromophenyl)pyrrolo[3,4-c]pyrrole-1,4(2H,5H)-dione (*5*)

3,6-Bis(4-bromophenyl)furo[3,4-c]furan-1,4-dione (**4**) (500 mg, 1.12 mmol), *p*-bromo-aniline (576 mg, 3.36 mmol), dicyclohexylcarbodiimide (692 mg, 3.36 mmol) and trifluoroacetic acid (6 μl, 0.07 mmol) were dissolved in 250 ml chloroform and stirred for 3 d at room temperature. The solvent was removed, and the residue washed with methanol. After filtering, the red coloured product was purified by column chromatography (toluene). The product was recrystallized from methanol as red crystals with a red solid state fluorescence. Yield: 466 mg (55%). ^{1}H NMR (400 MHz, $CDCl_3$): $\delta = 7.56$ (d, aromatic, 2H, $^{3}J = 8.7$ Hz), 7.51 (d, aromatic, 2H, $^{3}J = 8.9$ Hz), 7.48 (d, 2H, $^{3}J = 8.9$ Hz), 7.07 (d, aromatic, 2H, $^{3}J = 8.6$ Hz). ^{13}C NMR (100 MHz, $CDCl_3$): $\delta = 132.6, 132.0, 131.0, 129.1$. UV/Vis (dichloromethane): 338, 477, 503 nm.

2.4.2. 2,3,5,6-Tetrakis(4-(4-hexylthiophen-2-yl)phenyl)pyrrolo[3,4-c]pyrrole-1,4(2H,5H)-dione (***DPP1***)

In a vial, 150 mg (0.20 mmol) 2,3,5,6-tetrakis(4-bromophenyl) pyrrolo[3,4-c]pyrrole-1,4(2H,5H)-dione (**5**), 328 mg (1.00 mmol) 4-

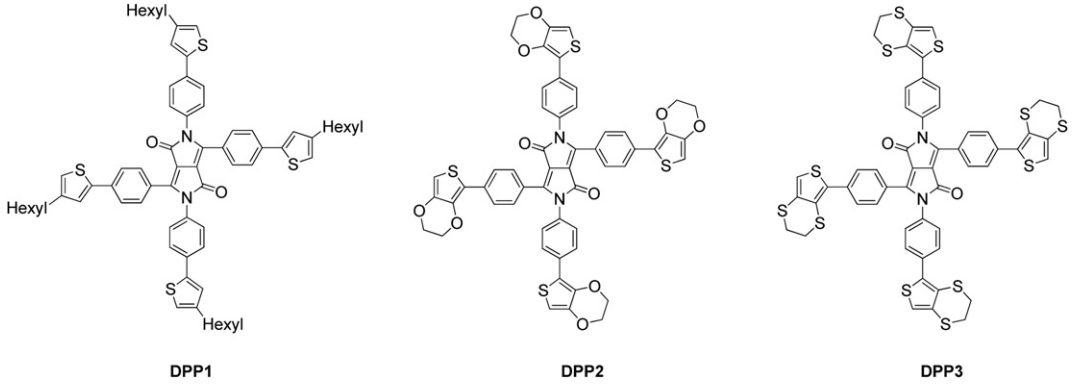

Fig. 2. Monomer structures **DPP1** – **DPP3**.

hexylthien-2-yl trimethylstannane, and 14 mg (0.012 mmol) tetrakis (triphenylphosphine) palladium(0) were dissolved in 5 ml dry DMF, and stirred for 5 min. The mixture was degassed, heated at 160 °C for 1 h in the microwave synthesizer. After cooling, the mixture was diluted with 75 ml dichloromethane, washed with 100 ml brine and 100 ml water. The organic layer was separated, dried over magnesium sulfate and evaporated. The red solid was recrystallized from dichloromethane/methanol. Yield: 190 mg (86%). ^{1}H NMR (400 MHz, $CDCl_3$): δ = 7.75 (d, aromatic, 4H, ^3J = 8.5 Hz), 7.65 (d, aromatic, 4H, ^3J = 8.0 Hz), 7.46 (d, aromatic, 4H, ^3J = 8.5 Hz), 7.20 (d, aromatic, 4H, ^3J = 8.5 Hz), 7.19 (d, aromatic, thienyl-, 2H ^4J = 1.39 Hz), 7.18 (d, aromatic, thienyl-, 2H, ^4J = 1.39 Hz), 6.91 (overlapping d, aromatic, thienyl-, 4H, ^4J = 1.39 Hz), 6.22 (q, CH_2—H, 8H), 1.64 (m, CH_2—H, 24H), 1.34 (m, CH_2—H, 8H), 0.98 (t, CH_3—H, 12H). ^{13}C NMR (100 MHz $CDCl_3$): δ = 161.54, 146.14, 144.16, 144.01, 142.31, 142.22, 136.78, 134.33, 125.48, 124.66, 110.20 (quaternary C); 129.94, 127.59, 125.73, 124.71 (aromatic CH); 125.33, 124.66, 120.64, 119.66 (thienyl- CH). UV/Vis (dichloromethane): 309, 395, 520 nm ε (520) = 7.3 × 10^3 L mol^{-1} cm^{-1}.

2.4.3. 2,3,5,6-Tetrakis(4-(2,3-dihydrothieno[3,4-b][1,4]dioxin-5-yl) phenyl)pyrrolo[3,4-c]-pyrrole -1,4(2H,5H)-dione (*DPP2*)

The procedure from compound (**DPP1**) was followed except that 3,4-ethylenedioxythien-2-yl trimethylstannane was used instead of 4-hexylthien-2-yl trimethylstannane, giving a dark red solid yielding 79%. ^{1}H NMR (600 MHz, DMSO-d_6): δ = 7.74 (d, aromatic, 4H, ^3J = 9.0 Hz), 7.68 (d, aromatic, 4H, ^3J = 9.0 Hz), 7.65 (d, aromatic, 4H, ^3J = 9.0 Hz), 7.29 (d, aromatic, 4H, ^3J = 9.0 Hz), 6.65 (s, EDOT aromatic H, 2H), 6.61 (s, EDOT aromatic H, 2H), 4.40–4.20 (m, EDOT—CH_2, 16H). ^{13}C NMR (150 MHz, DMSO-d_6): δ = 160.83, 145.67, 142.01, 141.99, 139.70, 138.74, 135.21, 133.52, 132.23, 124.56, 114.65, 114.59, 109.48 (quaternary C); 129.44, 128.07, 125.30, 124.20 (aromatic CH); 99.59, 98.23 (thienyl- CH); 64.55, 64.47, 63.75, 63.70 (EDOT-CH_2). UV/Vis (dichloromethane): 317, 535 nm ε (535) = 7.7 × 10^3 L mol^{-1} cm^{-1}.

2.4.4. 2,3,5,6-Tetrakis(4-(2,3-dihydrothieno[3,4-b][1,4]dithiin-5-yl) phenyl)pyrrolo[3,4-c] pyrrole-1,4(2H,5H)-dione (*DPP3*)

The procedure from compound (**DPP1**) was followed except that 3,4-ethylenedithiathien-2-yl trimethylstannane was used instead of 4-hexylthien-2-yl trimethylstannane, giving a dark solid. (81%). ^{1}H NMR (400 MHz, $CDCl_3$): δ = 7.85 (d, aromatic, 4H, ^3J = 8.5 Hz), 7.65 (d, aromatic, 4H, ^3J = 8.5 Hz), 6.68 (s, EDTT aromatic H, 2H), 3.24 (t, EDTT—CH_2, 8H), 3.80 (t, N—CH_2, 4H), 1.57 (m, CH, 2H), 1.14 (m, CH_2, 56H), 0.88 (t, CH_3, 12H). ^{13}C NMR (150 MHz, DMSO-d_6): δ = 160.69, 145.75, 135.36, 134.56, 133.11, 133.00, 132.37, 126.83, 126.48, 125.77, 123.82, 122.86, 110.01 (quaternary CH); 129.40, 128.24, 128.11, 127.07 (aromatic CH); 118.81, 117.97 (thienyl- CH); 27.48, 27.43, 26.52, 26.45 (EDTT-CH_2). UV/Vis (dichloromethane): 253, 309, 519 nm ε (519) = 5.3 × 10^3 L mol^{-1} cm^{-1}.

3. Results and discussion

3.1. Synthesis

The synthetic route for the starting compound 2,3,5,6-tetrakis-(4-bromophenyl) pyrrolo[3,4-c]pyrrole-1,4(2H,5H)-dione (**5**) and the key compounds **DPP1** – **DPP3** is described in Scheme 1. The intermediates ethyl 3-(4-bromophenyl)-3-oxopropanoate (**2**), diethyl 2,3-bis(4-bromobenzoyl)succinate (**3**) and 3,6-bis(4-bromophenyl) furo[3,4-c]furan-1,4-dione (**4**) were synthesized following literature procedures [15,27]. The synthesis of monomer **5** required a condensation reaction of the intermediate **4** with *p*-bromo-aniline, in

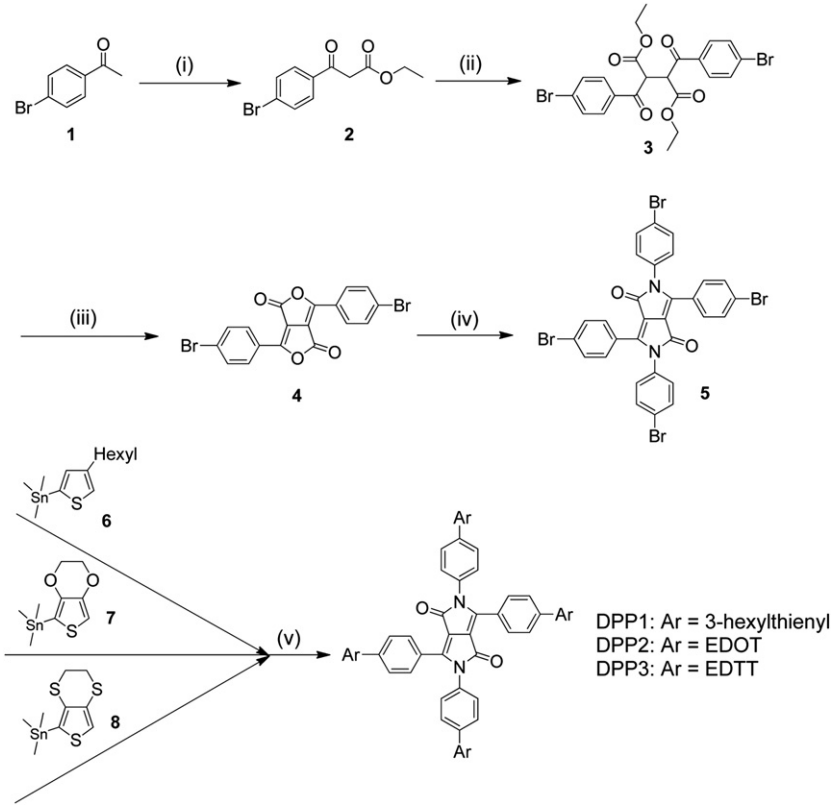

Scheme 1. Synthesis of tetrafunctionalized DPP monomers. Reagents and Conditions: (i) diethyl carbonate, NaH, toluene, reflux. (ii) (a) Br_2, $CHCl_3$; (b) NaH, diethyl ether, reflux. (iii) 200 °C, 20 min (iv) *p*-bromo-aniline, *N,N′*-dicyclohexylcarbodiimide, CF_3COOH, $CHCl_3$, 3d. (v) $Pd(PPh_3)_4$, dimethylformamide, microwave, 1 h.

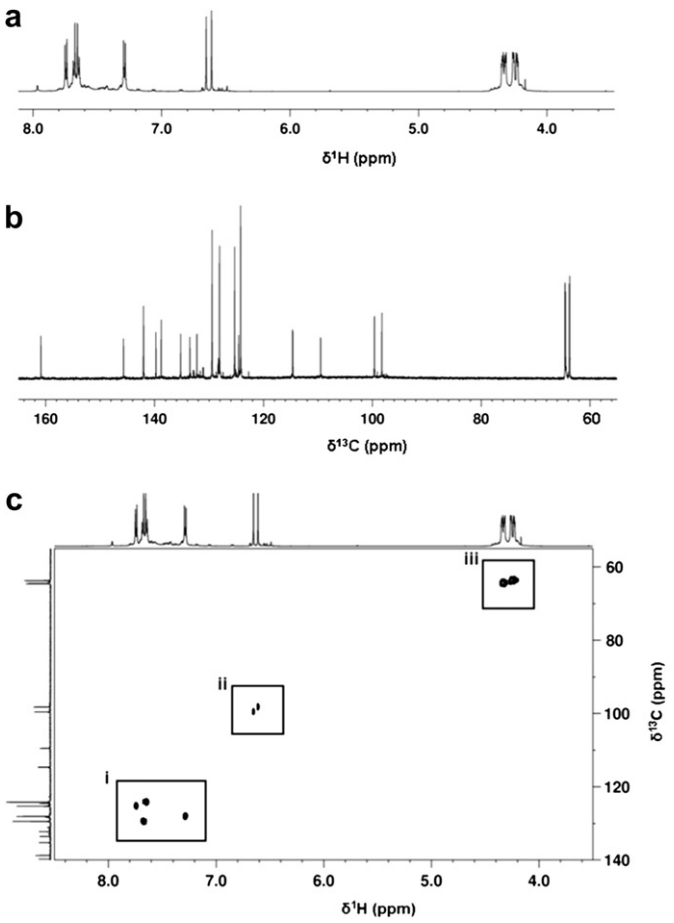

Fig. 3. NMR data for **DPP2** in DMSO-d_6 at 350 K acquired at a magnetic field strength of 14.1 T a) 1D ^{1}H NMR spectrum for the spectral region showing signals associated with the sample (solvent signal not shown). b) 1D ^{13}C–{^{1}H} UDEFT NMR spectrum in which signal intensities reflect relative number of centres associated with each signal. c) 2D [^{1}H, ^{13}C] HSQC NMR data which clearly reveals the relationship between ^{1}H and ^{13}C centres *via* $^{1}J_{CH}$ coupling. c) (i) aromatic CH correlations; c) (ii) thienyl CH correlations; c) (iii) EDOT bridge CH_2 correlations.

which the lactone units were converted into lactam units. A brilliant red solid product was obtained in 55% yield.

The 4-hexyl-thiophene-, 3,4-ethylenedioxythiophene- (EDOT-) and 3,4-ethylene dithiathiophene- (EDTT-) substituted monomers **DPP1**, **DPP2**, and **DPP3** were synthesized using a microwave assisted Stille coupling of monomer **5** with 4-hexylthien-2-yl trimethylstannane (**6**), 3,4-ethylenedioxythien-2-yl trimethylstannane (**7**) and 3,4-ethylene- dithiathien-2-yl trimethylstannane (**8**) using $Pd(PPh_3)_4$ as the catalyst and DMF as the solvent. The microwave assisted coupling methods gave high yields of 86, 71 and 81% for **DPP1**, **DPP2**, and **DPP3**, respectively. All the three monomers are red solids, which are soluble in common organic solvents such as chloroform, dichloromethane, DMF, THF and toluene, for example.

The ^{1}H and ^{13}C NMR data for **DPP1**, **DPP2**, and **DPP3** displayed all the expected resonances at the relevant chemical shifts with no discernible peaks corresponding to impurities. In order to achieve adequate ^{13}C signal-to-noise ratio for the relatively less soluble **DPP2** and **DPP3**, samples were solubilized in DMSO-d_6 with microwave assistance and data were acquired at 350 K and 150 MHz using a UDEFT approach. Under these conditions sufficient material was soluble and instrument conditions were such that adequate data were acquired to enable a ^{13}C signal count to be achieved. The 1D ^{1}H, ^{13}C–{^{1}H} UDEFT and 2D [^{1}H, ^{13}C] HSQC NMR data for **DPP2** are displayed in Fig. 3 by way of example. Symmetry considerations are such that half the number of signals appear for the number of centres in the molecules, but sufficient differences within each symmetry unit between similar functional groups enable unique chemical shifts to be discerned, underlining the sensitivity, particularly of ^{13}C chemical shifts, to remote influences of functional groups. In the case of each derivative the singlet signal at around 6.9 ppm can be ascribed to the thiophene unit in the 3-hexylthiophene-, EDOT- and EDTT- substituents. The two multiplets with a chemical shift of about 4.34 ppm (Fig. 3) are typical for the ethylene bridge of the EDOT unit in **DPP2**. In the case of the data for **DPP3**, the two triplet-like signals possessing a chemical shift of about 3.37 ppm are typical for the ethylene bridge of the EDTT unit with reference to the literature [29].

3.2. UV/vis absorption of monomers

The UV/vis absorption spectra of **DPP1**, **DPP2**, and **DPP3** are similar. Compared to the starting compound **5** (λ_{max} = 502 nm), bathochromic shifts are observed upon the addition of the thiophene derivatives to the conjugated system (Fig. 4a). While the EDOT-substituted monomer **DPP2** showed a large shift of 33 nm, the 4-hexylthienyl- and EDTT-substituted monomers **DPP1** and **DPP3** exhibit smaller shifts of 18 and 17 nm, respectively. The reason could be the weaker electron donating effect caused by sulfur in the EDTT unit compared to oxygen in the EDOT unit, which leads to a less extended conjugated system in **DPP3**. As for **DPP1**,

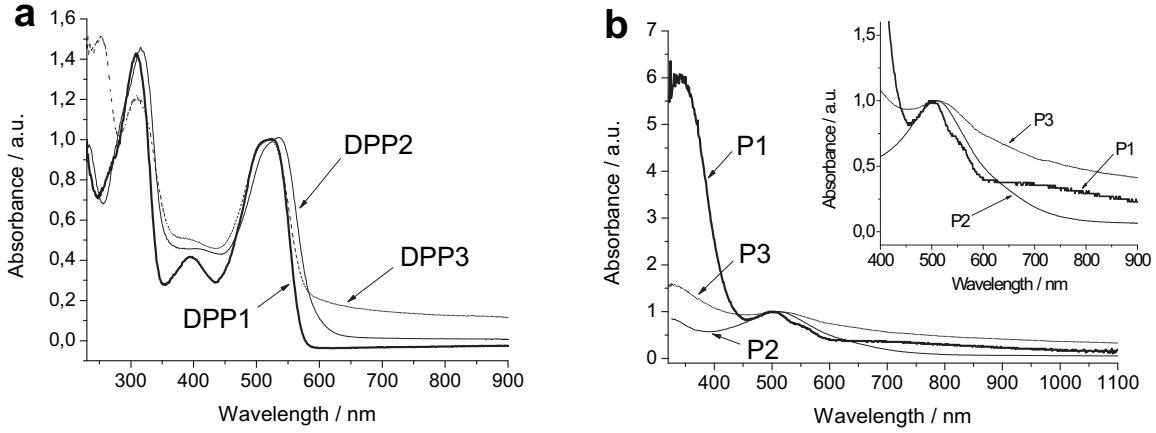

Fig. 4. UV/vis absorption spectra of monomers **DPP1** – **DPP3** (a). UV/vis absorption spectra of polymers **P1** – **P3** (b).

Table 1
Optical and electrochemical data for monomers[a] DPP1–DPP3 and Polymers[b] P1–P3.

	UV/nm	HOMO–LUMO gap/opt/eV	Onset of oxidation/V	HOMO/eV	Onset of reduction/V	LUMO/eV	HOMO–LUMO gap/eV
DPP1	309, 395, 520	2.17	+0.71	−5.51	−1.36	−3.44	2.07
DPP2	317, 535	2.11	+0.59	−5.39	−1.39	−3.41	1.98
DPP3	253, 309, 519	2.14	+0.59	−5.39	−1.41	−3.39	2.00
P1	342, 504	2.07	−0.09	−4.71	−1.01	−3.79	1.20
P2	510	1.72	−0.12	−4.68	−1.35	−3.45	1.23
P3	511	1.70	−0.25	−4.55	−1.23	−3.57	1.48

[a] Absorption spectra were taken in dichloromethane solutions.
[b] Absorption spectra were taken from films. All redox potentials are referenced to the ferrocene/ferrocenium redox couple. HOMO–LUMO gap according to the equation [31]: $-E_{LUMO} = E_{onset(red)} + 4.8$ eV and $-E_{HOMO} = E_{onset(ox)} + 4.8$ eV, where $E_{onset(ox)}$ and $E_{onset(red)}$ are the onset potentials for the oxidation and reduction processes vs. ferrocene.

3-hexylthiophene is not as electron rich as EDOT, which leads to a less extended conjugated system compared with **DPP2** with EDOT-substituent. The onset absorption edges of the monomers occur at about 580 nm, corresponding to optical HOMO–LUMO gaps in the range 2.11–2.17 eV (Table 1).

3.3. Electrochemistry

3.3.1. Electropolymerization

DPP1, **DPP2**, and **DPP3** were studied by cyclic voltammetry in dichloromethane solution using a glassy carbon working electrode, a platinum coil counter electrode, a Ag/AgCl reference electrode, and tetrabutylammonium hexafluorophosphate as the supporting electrolyte. The electropolymerization was carried out under potentiodynamic conditions. The data are collected in Table 1, the cyclic voltammograms are displayed in Fig. 5. The monomers exhibit quasi-reversible oxidation waves at about +0.80 V and reversible reduction peaks at about −1.45/−1.35 V, which gave HOMO–LUMO gaps of 2.07 eV for **DPP1**, 1.98 eV for **DPP2**, and 2.00 eV for **DPP3**. The values are in good agreement with the optically determined HOMO-LUMO gaps. Anodic oxidation of **DPP1** is indicated by two quasi-reversible peaks at +0.78 and +0.91 V, which could be caused by the two different thiophene-aryl-substituents in the 2,5- and 3,6-positions of the DPP core. **DPP2** and **DPP3**, however, only showed one oxidation peak at about +0.70 V. The broad shape of the peak suggests that it represents a superposition of two very close peaks of the EDOT-aryl- and EDTT-aryl-substituents in either the 2,5- or 3,6-position of the central DPP chromophore.

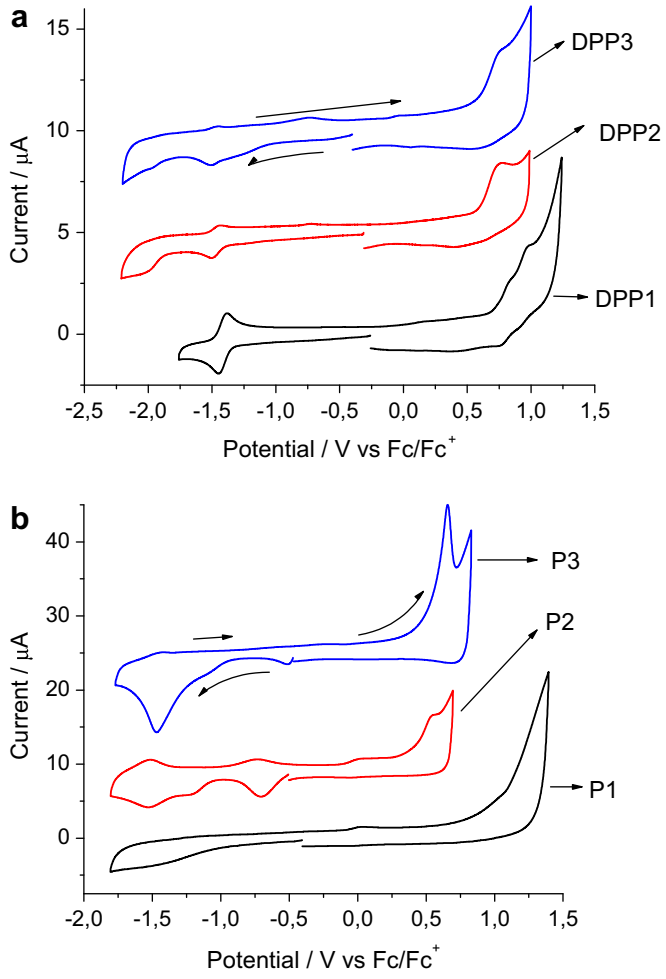

Fig. 5. Cyclic voltammograms of monomers **DPP1** – **DPP3** in solution (a) and polymers **P1** – **P3** as thin films deposited on a glassy carbon electrode. Solvent: 0.1 M $TBAPF_6$ in dichloromethane (a) or acetonitrile (b). Potential calculated versus ferrocene. Scan rate: 100 mV s^{-1}; $T = 20$ °C.

As shown in Fig. 6, the monomers were electropolymerized using the same solvent and conditions as for the cyclic voltammetry experiments, i.e., the potential was cycled repetitively over the redox-active range of the materials (from −0.25 to +1 V for **P1**, and from −0.30 to +0.80 V for **P2**, and from −0.375 to +0.875 V for **P3**, respectively). The polymer growth plots are displayed in Fig. 6. **DPP2** and **DPP3** polymerized readily, while **DPP1** required twice as many cycles, which could be caused by the high oxidation potential of mono-thiophene without electrodonating groups as in EDOT or EDTT [32], or as a consequence of the slow kinetics of chemical coupling for oxidized **DPP1**.

During the polymer growth many different signals appeared. This could be in accordance with the random growth of the polymers, which is obtained through all thiophene units (top/bottom to left/right), and not only through those in the 3- to 6-positions (left to right) or 2- to 5-positions (top to bottom). According to our previous paper [25], this could be likely because the thiophene units in the 3- (left) and 6- (right) positions are conjugated to each other meaning that any radical cation formed is stabilised and resonated over this conjugation before radical combination could allow polymer growth.

For the three materials, new peaks emerged at lower potentials, which is typical for growth and elongation of conjugated polymer main chains. The polymers exhibit HOMO–LUMO gaps in a range from 1.68 to 1.80 eV, which is lower than the insulating polymer only grown through the 2,5-positions ($E_g > 3$ eV).[25] For **DPP1**–**DPP3** the polymers are probably obtained with short conjugated chains, in which the conjugation in the network is broken by random 2.5- to 3,6-position (top–bottom) combinations.

The probabilities of formation of differently sized conjugated blocks are plotted in Fig. 7. The 'degree of polymerization' indicates the number of monomer units being connected to form the polymer chain, e.g., a degree of three indicates that the polymer chain consists of three monomer units. The term 'number of conjugated

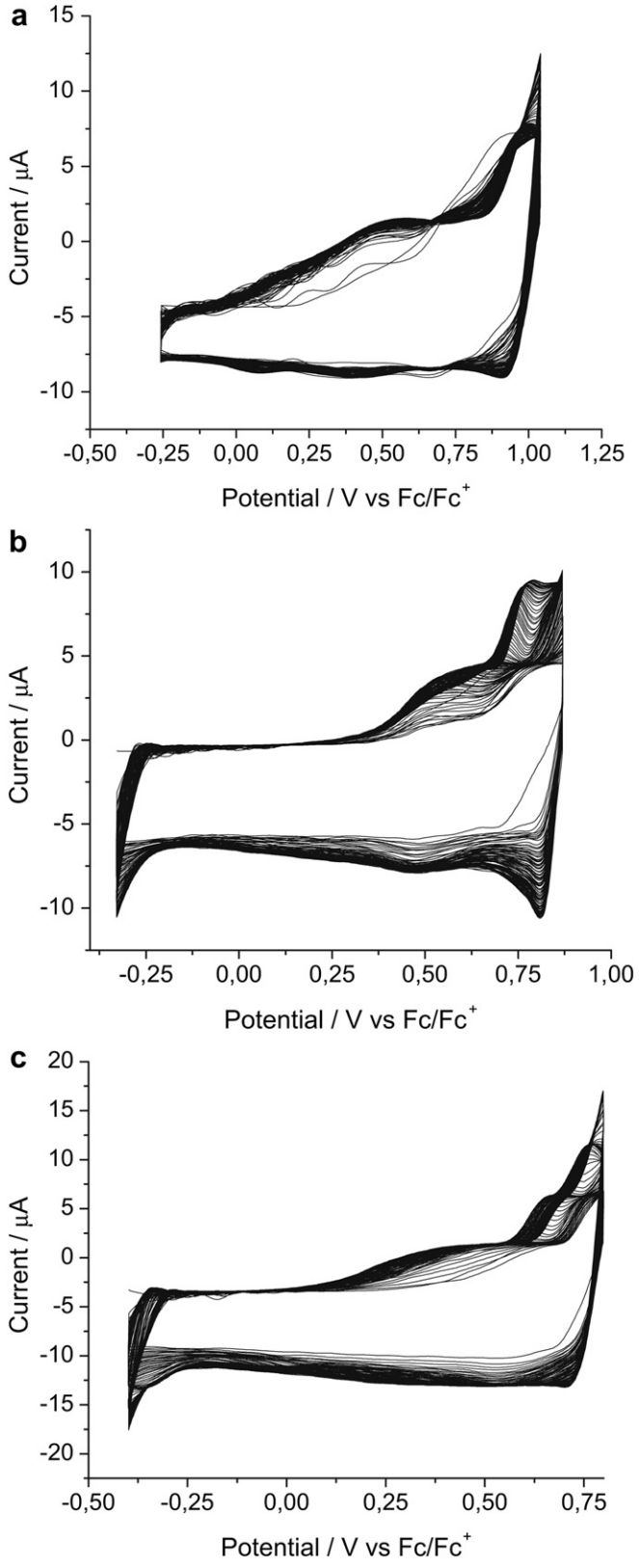

Fig. 6. Growth of **P1** (a), **P2** (b), and **P3** (c) by cyclic voltammetry in dichloromethane using a carbon working electrode, and Ag wire pseudo-reference electrode. 60 cycles were applied. Supporting electrolyte: 0.1 M $TBAPF_6$. Scan rate: 500 mV s^{-1}; $T = 20$ °C.

units' indicates, how many of the monomer units in the polymer chain are in π-conjugation with each other. For a chain with degree of polymerization of 2, four possibilities exist: The two monomers can be coupled via their b-positions (see Fig. 7a), a-positions, a- and b-, or b- and a-position. In the first case a conjugated dimer is obtained, the number n of conjugated units is 2. In the second case, a fully non-conjugated dimer is formed, n is zero. In the third and fourth case one of the 2 units is conjugated and the other one is not, n is 1. For $n = 2$ and $n = 0$, the probabilities are 25% each, for $n = 1$ it is 50%. In Fig. 7b the probability is plotted versus the number n of conjugated units for different degrees of polymerization. It is shown, for example that in a polymer with degree of polymerization of five the presence of an isolated conjugated unit ($n = 1$) exhibits 58% probability, whereas the existence of conjugated dimers, trimers, and tetramers only has 25, 12, and 6% probability, respectively. The formation of a fully conjugated or non-conjugated chain is the least probable scenario (Fig. 7b). Fig. 6c indicates that there is little change in the probabilities of differently sized conjugated blocks with increasing degree of polymerization.

3.3.2. Cyclic voltammograms of polymers

The electrochemistry of the electrochemically grown polymer films was investigated in acetonitrile vs. Ag/AgCl. The cyclic voltammograms of **P1**, **P2**, and **P3** are shown in Fig. 5(b) and the electronic data are listed in Table 1. **P1** exhibits irreversible oxidation and reduction waves, from which a HOMO–LUMO gap of 1.20 eV can be calculated. The diagram of **P2** is complex. The oxidation first shows a small and broad peak at low potential (0.12 V), which could be from bis-EDOT units in the 3- and 6-positions (left to right) of the chain, and the wave at higher potential (+0.54 V) indicating the oxidation of the EDOT units in the 2- and 5-positions (top to bottom). It is possible that the large reduction peak at (−0.70 V) could be the reverse of the oxidation process, but the peak itself shows some reversibility which makes the assignment of this peak ambiguous. The reduction of **P2** includes a reversible peak at −1.53/−1.51 V which is the same reduction process of the core seen in the monomer reduction (**DPP2**). There is also a shoulder at −1.30 V, which could be the reduction of a short conjugated chain. A HOMO–LUMO gap of 1.23 eV was determined. **P3** produced a less complex cycle. Upon anodic oxidation, a large irreversible wave emerge at +0.66 V, and upon reduction, an irreversible wave appeared at −1.45 V. A much smaller redox couple occured at −0.28/−0.51 V, which could indicate the same process as shown for **P2**, in which the conjugated units became oxidized. The other difference between the two polymers is the small peak at +0.01 V in **P2** (possibly being due to bis-EDOT) is absent in **P3** and this could be indicative of poor conjugation between two EDTT units which are twisted in relation to each other and therefore poor electron donors. [33] Finally, the reduction of the DPP core is irreversible in the case of **P3**. The HOMO–LUMO gap was determined as 1.48 eV.

3.3.3. UV/vis spectroscopic and spectroelectrochemical studies

It is of interest to study the spectroelectrochemical properties for this series of polymers. Thin polymer films were grown on ITO and electronic absorption spectra were taken. The 3-D electronic absorption plots for **P1**, **P2** and **P3** are shown in Fig. 8, the absorption data are listed in Table 1. In addition to the UV/vis absorption maxima at 504 nm for **P1**, 510 nm for **P2,** and 511 nm for **P3**, all three polymers showed broad shoulders from about 600–800 nm indicating an elongation of the π–π*-conjugated system along the polymer main chain. The spectroelectrochemistry of **P1** showed very little change until a potential of +1.3 V was reached. At this point there was a decrease in the π–π* transition.

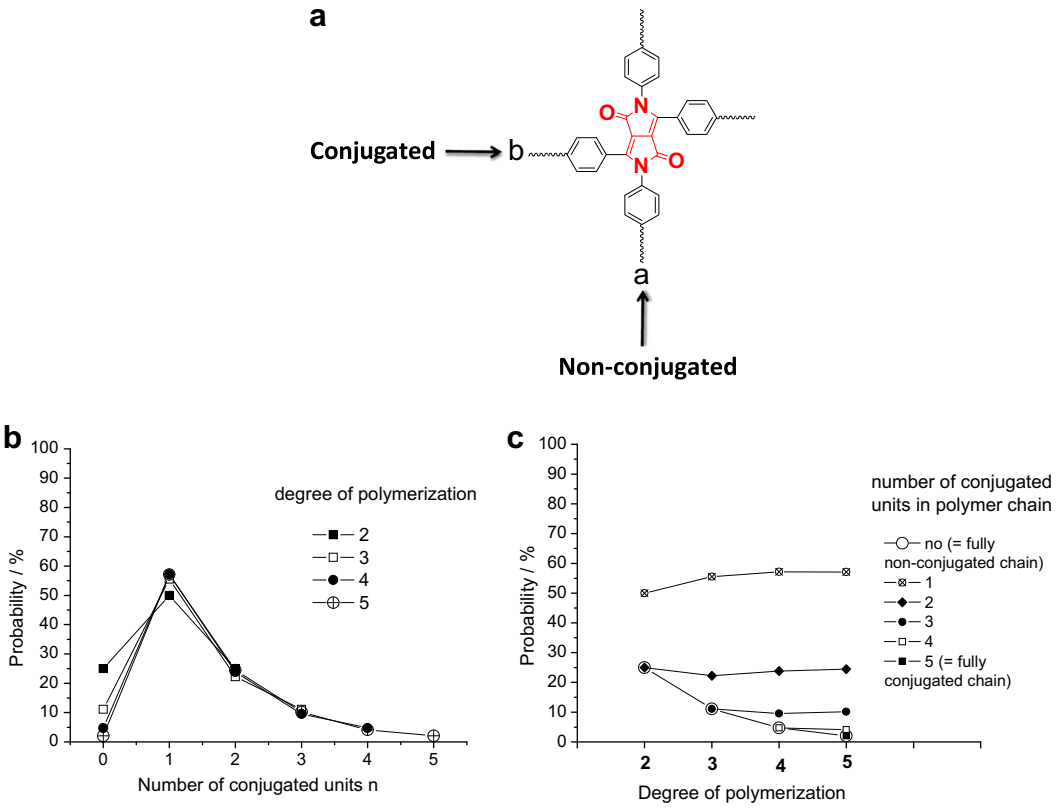

Fig. 7. Probabilities study for differently sized conjugated blocks.

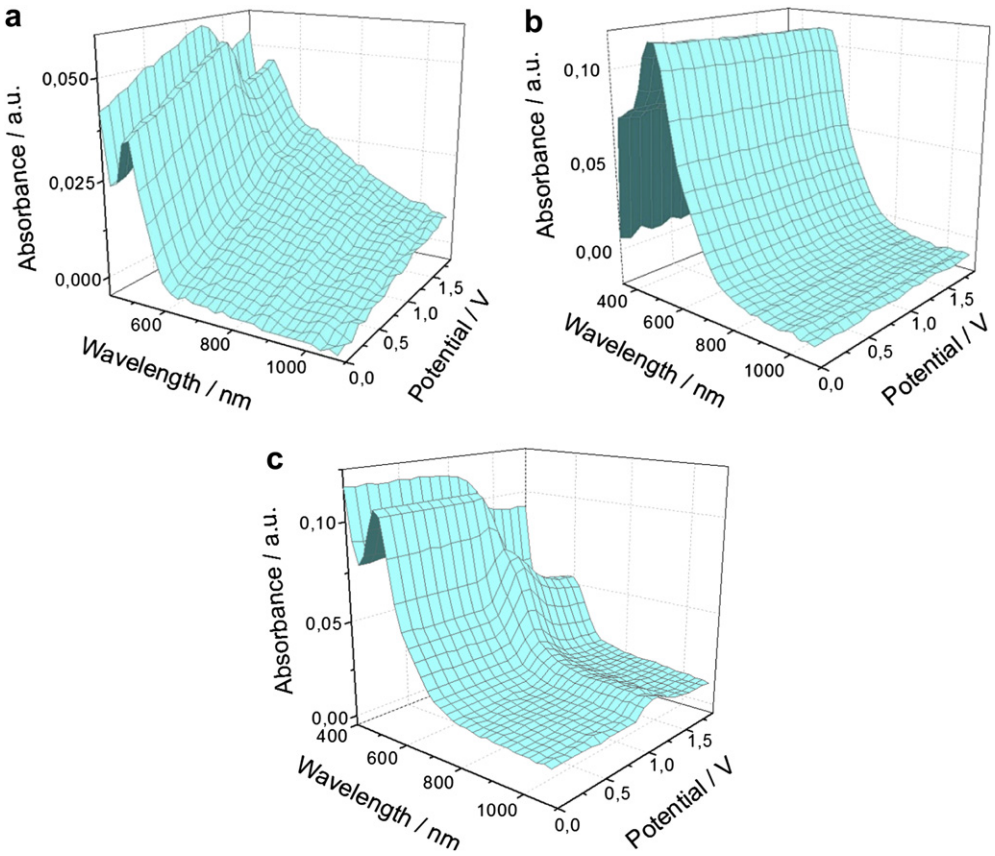

Fig. 8. Absorption spectroelectrochemical plots for **P1**, **P2**, and **P3** as thin films on ITO. Ag wire pseudo-reference electrode. Solvent: 0.1 M $TBAPF_6$ in acetonitrile. Potential calculated versus ferrocene. Scan rate: 100 mV s^{-1}; $T = 20$ °C.

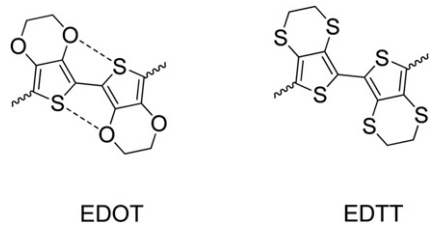

Fig. 9. Sulfur oxygen interaction between adjacent EDOT and EDTT units.

The broad absorption shoulder of **P1** starting from 650 nm increased. In a comparison, **P2** showed no change in the absorption characteristics with increasing p-doping. It could be possible that the polymer produced was highly cross-linked and, due to S–O interactions adjacent monomer units were densely packed so that counter ions could not diffuse into the film, balance the charge, and allow any change to occur (Fig. 9) [33].

The spectroelectrochemistry experiment for **P3** showed significant changes in the electronic absorption spectra with increasing potential. At +1.0 V, one can see the formation of polarons and bipolarons in the polymer chain which results in a new peak between 500 and 700 nm, followed by a drop in absorbance of the peak at 510 nm. Between +1.0 and +1.4 V there was a weak broad peak appearing from 700 nm. The S–O interaction between the adjacent EDOT units in **P2** does not exist in **P3**, so the EDTT-containing polymer is less likely to be densely packed, allowing easier access for the counter ions to diffuse into the polymer to balance the charge.

The reasoning for the large discrepancy between the optically and electrochemically determined band gaps is supported by the spectroelectrochemical results. For all three polymers, there is relatively little change in the absorption spectra and this indicates that oxidation takes place at localized, short-conjugation sites. The LUMO of the materials is therefore dominated by the DPP core and the HOMO is derived from the thiophene segments. The absorption spectra provide information about the $\pi-\pi^*$ transitions and the corresponding orbitals are clearly not representative of the HOMO and LUMO orbitals (since the gaps determined by the two methods differ by 0.2–0.9 eV). In conjugated polymers, this situation often arises when there is a strongly redox-active unit in the structure which is poorly conjugated to the main chain [34].

As an interesting comparison, the linear polymers containing 2,5-bis(4′-*t*-butylphenyl)-3,6-diphenylpyrrolo[3,4-c]pyrrole-1,4(2H,5H)-dione [25] with EDOT only attached to the 3,6-positions showed fully reversible oxidative and reductive waves. The polymer was fully conjugated and electrochromic, giving a HOMO–LUMO gap of 1.32 eV. The other polymer containing DPP units with EDOT only attached to the 2,5-positions showed irreversible oxidative and reductive waves, giving a HOMO–LUMO gap of 3 eV. This polymer was not conjugated and electrochromic. The observed behaviour suggests that the three polymers **P1**, **P2** and **P3** are not fully conjugated through the four cross-linked 2,3,5,6-directions.

4. Conclusion

In summary, a series of electropolymerizable tetrafunctionalized DPP monomers have been synthesized, and the corresponding polymers have been prepared upon anodic electropolymerization. The study shows that the polymer growth takes place randomly through the 2-, 3-, 5-, and 6-position of the DPP core. Compared with the monomers, **P1**, **P2** and **P3** showed broad longer wavelength absorption bands, which indicates an enlargement of the $\pi-$conjugation in the polymers. However, compared with linear polymers only grown through the 3,6-positions, the tetrafunctionalized monomers lead to polymers with less $\pi-$conjugation and only little pronounced electrochromic properties.

In polymers **P1**, **P2** and **P3**, conjugated blocks through coupling of thiophene units in the 3,6-positions were obtained, which are separated by non-conjugated blocks. As a result, the polymers are not as fully conjugated as the linear polymers prepared previously through coupling in the 3,6-positions.

Acknowledgements

Financial support by Ciba Specialty Chemicals, Basle, Switzerland, is gratefully acknowledged. Drs. M. Düggeli and R. Lenz from Ciba are kindly thanked for helpful discussions.

References

[1] Kraft A, Grimsdale AC, Holmes AB. Angew Chem Int Ed 1998;47:402.
[2] McGehee MD, Heeger AJ. Adv Mater 2000;12:1655.
[3] Günes S, Neugebauer H, Sariciftci NS. Chem Rev 2007;107:1324.
[4] Coakley KM, McGehee MD. Chem Mater 2004;16:4533.
[5] Murphy AR, Fréchet JMJ. Chem Rev; 2007:1066.
[6] Zaumseil J, Sirringhaus H. Chem Rev 2007;107:1296.
[7] Cicoira F, Santato C. Adv Funct Mater 2007;17:3421.
[8] Thomas SW, Joly GD, Swager TM. Chem Rev 2007;107:1339.
[9] Monk PMS, Mortimer RJ, Rosseinsky DR. Electrochromism: fundamentals and applications. Weinheim, Germany: VCH; 1995.
[10] Granqvist CG. Sol Energy Mater Sol Cells 2000;60:201.
[11] Granqvist CG, Avendano E, Azens A. Thin Solid Films 2003;442:201.
[12] Faughnan BW, Crandall RS, Heyman PM. RCA Rev 1975;36:177.
[13] Hao Z, Iqbal A. Chem Soc Rev 1997;26:203.
[14] Iqbal A, Jost M, Kirchmayr R, Pfenniger J, Rochat A, Wallquist O. Bull Soc Chim Belg 1988;97:615.
[15] Langhals H, Grundel T, Potrawa T, Polborn K. Liebigs Ann; 1996:679.
[16] Lange G, Tieke B. Macromol Chem Phys 1999;200:106.
[17] Song B, Wei H, Wang Z, Zhang X, Dehaen W. Adv Mater 2007;19:416.
[18] Chan W-K, Chen Y, Peng Z, Yu L. J Am Chem Soc 1993;115:11735.
[19] Beyerlein T, Tieke B. Macromol Rapid Commun 2000;21:182.
[20] Rabindranath AR, Zhu Y, Heim I, Tieke B. Macromolecules 2006;39:8250.
[21] Zhu Y, Heim I, Tieke B. Macromol Chem Phys 2006;207:2206.
[22] Cao D, Liu Q, Zheng W, Han S, Peng J, Liu S. J Polym Sci Pt A: Polym Chem 2006;44:2395.
[23] Beyerlein T, Tieke B, Forero-Lenger S, Brütting W. Synth Met 2002;130:115.
[24] Cao D, Liu Q, Zheng W, Han S, Peng J, Liu S. Macromolecules 2006;39:8347.
[25] Zhang K, Tieke B, Forgie JC, Skabara PJ. Macromol Rapid Commun 2009;30:1834.
[26] Zhu Y, Zhang K, Tieke B. Macromol Chem Phys 2009;210:431.
[27] Zhang K, Tieke B. Macromolecules 2008;41:7287.
[28] Groenendaal L, Jonas F, Freitag D, Pielartzik H, Reynolds JR. Adv Mater 2000;12:48.
[29] Crouch DJ, Skabara PJ, Lohr JE, McDouall JJW, Heeney M, McCulloch I, et al. Chem Mater 2005;17:6567.
[30] Piotto M, Bourdonneau M, Elbayed K, Wieruszeski J-M, Lippens G. Magn Reson Chem 2006;44:943–7.
[31] Bredas JL, Silbey R, Boudreux DS, Chance RR. J Am Chem Soc 1983;105:6555.
[32] Roncali J, Garreau R, Yassar A, Marque P, Garnier F, Lemaire M. J Phys Chem 1987;91:6706.
[33] Spencer HJ, Skabara PJ, Giles M, McCulloch I, Coles SJ, Hursthouse MB. J Mater Chem 2005;15:4783.
[34] Skabara PJ, Berridge R, McInnes EJL, West DP, Coles SJ, Hursthouse MB, et al. J Mater Chem 2004;14:1964.